Vailable online at www.sciencedirect.com

SciVerse ScienceDirect

Energy Procedia 27 (2012) 197 – 202

Energy Procedia

SiliconPV: April 03-05, 2012, Leuven, Belgium

Optimization of Rear Point Contact Geometry by Means of 3-D Numerical Simulation

R. De Rose[a,b]*, K. Van Wichelen[c], L. Tous[c], J. Das[c], F. Dross[c], C. Fiegna[a], M. Lanuzza[b], E. Sangiorgi[a], A. Uruena De Castro[c], M. Zanuccoli[a]

[a]*ARCES-DEIS, University of Bologna and IUNET, 47521 Cesena (FC), Italy*
[b]*DEIS, University of Calabria, 87036 Rende (CS), Italy*
[c]*IMEC, Kapeldreef 75, 3011 Heverlee, Belgium*

Abstract

In this work three-dimensional (3-D) numerical simulations, validated by the experimental measurements of a reference cell, have been performed to optimize the rear contact geometry of a PERC-type solar cell, featuring a high sheet resistance (140 Ω/sq) phosphorus-doped emitter and a front-side metallization with narrow and highly-conductive electro-plated copper lines (40 µm wide) on lowly resistive Ti contacts. The simulation results show that an optimization of the rear point contact design potentially leads to an efficiency improvement of 0.68%$_{abs}$ compared to the reference cell.

© 2012 Published by Elsevier Ltd. Selection and peer-review under responsibility of the scientific committee of the SiliconPV 2012 conference. Open access under CC BY-NC-ND license.

Keywords: Si solar cells; 3-D device simulation; PERC; high sheet resistance emitter; electro-plated Cu contacts

1. Introduction

Mono-crystalline Cz silicon full-metallized aluminum back surface field (full Al-BSF) solar cells with screen-printed front silver contacts and a standard 65-70 Ω/sq phosphorus-doped emitter exhibits a conversion efficiency around 18.5% [1]. Two of the most promising approaches to enhance the performance of Si solar cells are the optimization of the rear contact design and the development of technological solutions for contacting high sheet resistance emitters. It has already been widely demonstrated that the adoption of the PERC (Passivated Emitter and Rear locally Contacted) design with

* Corresponding author. Tel: +39-0547-338965; fax: +39-0547-339533
E-mail address: rderose@arces.unibo.it

1876-6102 © 2012 Published by Elsevier Ltd. Selection and peer-review under responsibility of the scientific committee of the SiliconPV 2012 conference. Open access under CC BY-NC-ND license.
doi:10.1016/j.egypro.2012.07.051

local point Al contacts at the rear side can boost the efficiency well above 19% [2]. As reported in [3], further improvements can be obtained by two means. First, introducing a high sheet resistance phosphorus-doped emitter with a low surface concentration is beneficial in order to reduce surface and Auger recombination at the front-side, leading to higher J_{sc} and V_{oc}. Second, by replacing the relatively wide screen-printed silver front-side fingers with narrower, denser and better conducting Ti/Cu electro-plated lines, front contact shadowing and the resistive losses can be reduced.

In this paper numerical device simulations have been performed by using a TCAD simulator [4] to optimize the rear point contact geometry of a PERC-type solar cell featuring a 140 Ω/sq phosphorus-doped emitter and electro-plated Ti/Cu front contacts (40 µm wide). As discussed in [5], due to the complexity of the geometry and to the presence of several competing physical mechanisms, a careful analysis and optimization of the rear point contact design require a rigorous three-dimensional (3-D) modeling approach. The optimization of the rear contact geometry has been performed by changing the rear contact pitch and by considering a constant rear contact diameter of 35 µm. The size of the rear contacts is set consistently with the technological limitation of the laser rear patterning process used to form local contact holes [3][6].

2. Experimental and simulation data

The reference PERC cell (size 12.5x12.5 cm^2, semi-square) features a 1.3 Ω cm, 150 µm thick *p*-type Si-Cz substrate and a random pyramid textured front surface with a 80 nm thick SiN_x anti-reflective coating (ARC) layer. The front-side electro-plated Ti/Cu contacts are 40 µm wide with a thickness of 9 µm and a pitch of 1.53 mm. The rear-side metallization consists of local Al contact holes with a diameter of 35 µm and a pitch of 550 µm, while the rear passivation layer features a SiO_2/SiN_x stack. A local Al-BSF is formed in the openings by firing the rear Al layer. For further details on the process and the design of the reference PERC-type cell, refer to [6]. The performance of this reference cell has been measured and summarized in Table 1. The related illuminated I-V curve is shown in Fig. 1.

Table 1. Performance of the experimental and simulated PERC cells

Cell type	V_{oc} (mV)	J_{sc} (mA/cm^2)	*FF* (%)	η (%)
Measured	653.7	38.9	77.0	19.6
Simulated	653.6	38.9	77.1	19.6

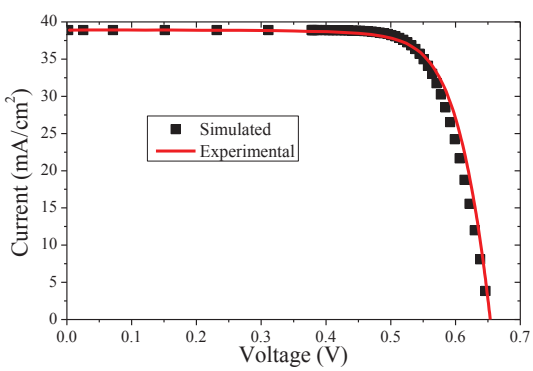

Fig. 1. Experimental vs. simulated illuminated I-V curve for the reference PERC cell

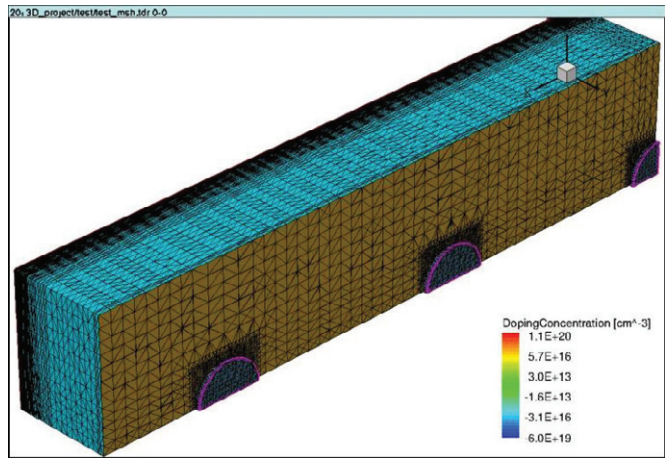

Fig. 2. 3-D simulated structure of the reference PERC cell (back view)

The 3-D simulated structure, built and configured on the basis of the characteristics of the reference cell, is shown in Fig. 2. For symmetry purposes, the rear contact pitch of the simulated cell is set to 510 μm to make sure that the ratio between the front contact pitch (1.53 mm) and the rear hole pitch is an integer number. Under this assumption, the lateral size and depth of the 3-D simulation domain can be limited respectively to the half of the front finger pitch and the half of the rear contact pitch, while the height is equal to the substrate thickness [5]. This allows reducing the simulation run-time for the I-V characteristics to ~3 hours with a 3-D simulation domain for the reference cell featuring about 230000 grid nodes on a 8-core Intel Xeon X53xx processor.

An ad-hoc calibration of the physical parameters and models has been performed to obtain realistic predictions in the optimization procedure. The main critical parameters of the simulated reference PERC cell are summarized in Table 2. The adopted models include the Schenk band-gap narrowing model to account for the effective intrinsic density [7], the surface doping-dependent front surface recombination velocity (SRV) according to [8][9] and the doping-dependent mobility model proposed by Klaassen [10][11]. Fermi-Dirac statistics has been adopted to properly model the highly-doped regions (emitter and BSF) within the device. The SRV at the rear passivated surfaces is set to 330 cm/s, while the front/rear contact SRV at electrodes is assumed to be $2x10^6$ cm/s, similarly to that used in [3][6]. It is worth noting that the assumed values for the SRV at rear passivated and metallized surfaces and the rear metallization fraction strongly impact on the effective rear surface recombination velocity and consequently on the performance of a locally contacted rear surface passivated solar cell, as well described in [12][13].

The optical simulation has been performed at 1-sun illumination condition with a Ray Tracer tool in the TCAD simulator**,** accounting for the front texturing and ARC layer and for the different reflectivity at the rear passivated (0.9) and metallized surfaces (0.65) [14].

The 140 Ω/sq phosphorus-doped emitter is modeled by a Gaussian function with a peak concentration of $2x10^{19}$ cm^{-3} and a junction depth of 0.6 μm. All the series parasitic resistance losses (including the front and the rear contact resistance and the front metal resistance) have been accounted by a post-processing analysis. The shunt resistance and the busbars resistance have been neglected. It is worth noting that the non-ideal resistive-limited enhanced recombination effects (giving a local non-ideality factor n2>2) [6] are not taken into account.

The simulated performance and I-V curve for the reference cell are reported in Table 1 and Fig. 1, respectively. A good agreement can be observed between experimental and simulated results.

Table 2. Parameters of the simulated reference PERC cell

Parameter	*value*	*units*
Front contact pitch	1530	μm
Front finger length	12.3	cm
Rear contact pitch	510	μm
Rear contact fraction	0.37	%
Rear passivation SRV	330	cm/s
Front/rear contact SRV	$2x10^{6}$	cm/s
Bulk lifetime	500	μs
Front metal resistivity	$1.8x10^{-6}$	Ω cm
Front contact resistivity	$5x10^{-4}$	Ω cm^2
Rear contact resistivity	$1x10^{-3}$	Ω cm^2

3. Rear contact design optimization

The optimization of the PERC cell has been performed in terms of rear contact pitch, keeping the diameter of the rear hole contacts constant (35 μm). The simulation results for the short-circuit current density (J_{sc}), the open-circuit voltage (V_{oc}), the fill factor (FF) and the efficiency (η) as a function of the rear contact fraction (CF_{rear}), defined as the ratio of the rear contacted area to the total cell area, are plotted in Fig. 3.

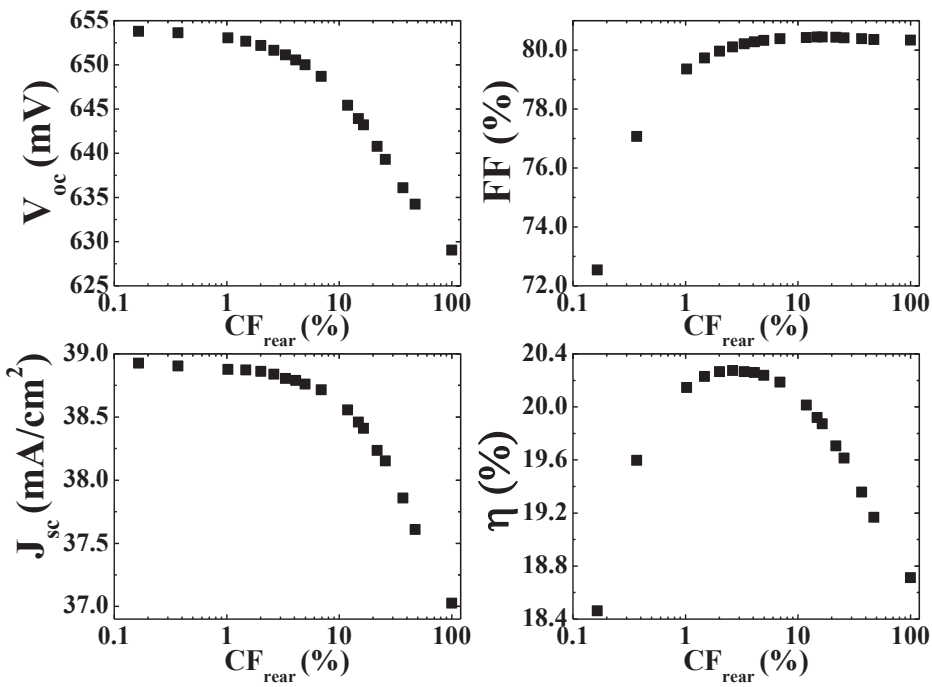

Fig. 3. Simulation results for the optimization of rear point contact geometry in terms of rear contact pitch

Table 3. Simulation results for the reference, the optimal and the rear full-metallized cells

Cell type	CF_{rear} (%)	V_{oc} (mV)	J_{sc} (mA/cm^2)	FF (%)	η (%)
Reference	0.37	653.63	38.90	77.07	19.60
Optimal	2.63	651.64	38.84	80.11	20.28
Rear full-metallized	100	629.06	37.03	80.34	18.71

As expected, by decreasing the CF_{rear}, both J_{sc} and V_{oc} increase due to the reduction of the effective rear surface recombination velocity and to the increase of the effective internal bottom reflectivity. On the contrary, an opposite trend can be observed for the FF: by decreasing the CF_{rear}, the base spreading resistance and the rear contact resistance increase, leading to a strong degradation of the FF at CF_{rear}< 1%. The efficiency trade-off due to these opposite trends leads to an optimal value of CF_{rear} within the range 2-3%. It is worth noting that the obtained optimum value of CF_{rear} is influenced by several factors: among them, the assumed SRV values at rear metallized and passivated surfaces, the substrate resistivity and the size of the rear point contacts. Concerning the hole contact diameter, it has already been shown in [15] that the optimization of PERC-type solar cells depends on the size of the rear point contacts. In particular, for a given rear contact fraction, a smaller hole diameter means a smaller distance between adjacent rear contacts, leading to higher efficiency because of a reduced base spreading resistance. Moreover, a smaller hole contact diameter leads to a lower optimum value of CF_{rear}, as reported in [15].

In Table 3 the simulation results obtained for the reference cell (CF_{rear}= 0.37%), for the optimal cell (CF_{rear}= 2.63%, equivalent to a rear contact pitch of 191.25 μm) and for the rear full-metallized cell (CF_{rear}= 100%) are compared. The simulation results show that the optimization of the rear point contact design for the analyzed PERC cell can potentially lead to an efficiency improvement of 0.68%$_{abs}$ compared to the reference cell and of 1.57%$_{abs}$ with respect to the case of full-metallized rear side, resulting in a conversion efficiency above 20%.

4. Conclusions

In this work a rigorous 3-D modeling approach has been adopted for representing an advanced PERC-type solar cell, featuring a high sheet resistance (140 Ω/sq) phosphorus-doped emitter and front-side 40 μm wide electro-plated Ti/Cu contacts. 3-D numerical device simulations, validated by the experimental measurements of a reference cell, have been performed to optimize the rear contact geometry of the analyzed PERC cell. The simulation results show that such optimization can potentially leads to an efficiency improvement of 0.68%$_{abs}$ compared to the reference cell, achieving a conversion efficiency above 20%.

References

[1] International Technology Roadmap for Photovoltaic (ITRPV.net), 2010, http://www.itrpv.net.

[2] V. Prajapati , J. John, X. Yang, W. Mischke, J. Hong. Silane free high-efficiency industrial silicon solar cells using dielectric passivation and local BSF. *Proc. of 25th EU PVSEC*, Valencia, Spain, 2010, pp. 1469-1474.

[3] K. Van Wichelen, L. Tous, A. Tiefenauer, C. Allebé, T. Janssens, P. Choulat, J. L. Hernandez, E. Cornagliotti, M. Debucquoy, A. Ruocco, J. John, P. Verlinden, F. Dross, K. Baert. Towards 20.5% efficiency PERC cells by improved understanding through simulation. *Energy Procedia* 8 (2011), pp. 78-81.

[4] Sentaurus-Device, Synopsys Inc., Mountain View, CA. URL: www.synopsys.com/products/tcad.

[5] M. Zanuccoli, R. De Rose, P. Magnone, M. Frei, H.-W. Guo, M. Agrawal, E. Sangiorgi, C. Fiegna. Numerical Simulation and Modeling of Rear Point Contact Solar Cells. *Proc. of 37th IEEE Photovoltaic Specialists Conference (PVSC)*, Seattle, WA, USA, 2011, pp. 1519-1523.

[6] C. Allebé, L. Tous, K. Van Wichelen, J. L. Hernandez, M. Aleman, M. Ngamo, J. Poortmans, R. Mertens. Large-area PERC cells with a Ti-Cu based metallization leading to efficiencies above 19.5%. *Proc. of 26th EU PVSEC*, Hamburg, Germany, 2011.

[7] A. Schenk. Finite-temperature full random-phase approximation model of band gap narrowing for silicon device simulation. *Journal of Applied Physics* 84 (7), 1998, pp. 3684-3695.

[8] M. J. Kerr. Surface, emitter and bulk recombination in silicon and development of silicon nitride passivated solar cells. *PhD thesis*, Australian National University, 2002.

[9] P. P. Altermatt, J. O. Schumacher, A. Cuevas, M. J. Kerr, S. W. Glunz, R. R. King, G. Heiser, A. Schenk. Numerical modeling of highly doped Si:P emitters based on Fermi-Dirac statistics and self-consistent material parameters. *Journal of Applied Physics* 92 (6), 2002, pp. 3187-3197.

[10] D. B. M. Klaassen. A unified mobility model for device simulation: I. model equations and concentration dependence. *Solid-State Elec.* 35 (7), 1992, pp. 953-959.

[11] D. B. M. Klaassen. A unified mobility model for device simulation: II. temperature dependence of carrier mobility and lifetime. *Solid-State Elec.* 35 (7), 1992, pp. 961-967.

[12] A. Wolf, D. Biro, J. Nekarda, S. Stumpo, A. Kimmerle, S. Mack, R. Preu. Comprehensive analytical model for locally contacted rear surface passivated solar cells . *Journal of Applied Physics* 108 (12), 2010, pp. 124510-13.

[13] P. Saint-Caste, D. Biro, J. Nekarda, S. Stumpo, A. Kimmerle, S. Mack, R. Preu. Comprehensive analytical model for locally contacted rear surface passivated solar cells . *Journal of Applied Physics* 108 (1), 2010, pp. 013705-7.

[14] Synopsys. Optimization of Rear Contact Design in Monocrystalline Silicon Solar-Cell Using 3D TCAD Simulations. *TCAD Sentaurus application note*, July 2010.

[15] M. Zanuccoli, R. De Rose, P. Magnone, E. Sangiorgi, C. Fiegna. Performance Analysis of Rear Point Contact Solar Cells by Three-Dimensional Numerical Simulation. *IEEE Transactions on Electron Devices* 59 (5), 2012, pp. 1311-1319.